

铜离子配位调控的 TICT 荧光化合物的双重荧光发射

张静丽 范伟贞 闫素婷 林丽榕* 黄荣彬

(厦门大学化学化工学院, 厦门 361005)

摘要: 设计合成了 2 个分子内扭转电荷转移(TICT)荧光体(**1** 和 **2**), 铜离子的配位作用可开关其双重荧光发射。**2** 在乙腈/水溶液(1:1, V/V)中的双重荧光发射随着铜离子的加入以类似电子转移机制“开-关”形式猝灭, 而 **1** 在铜离子与其计量比为 1 之内的乙腈/水溶液(1:1, V/V)中, 其双重荧光发射随着铜离子的加入逐渐猝灭; 在计量比之后其长波长的 TICT 荧光发射随着铜离子的加入逐渐增强。即 **1** 的 TICT 荧光发射以“开-关-开”的机制被铜离子诱导。同时还获得了铜离子与 **1** 形成的配合物的晶体结构以及配合物的荧光性质。¹H NMR 波谱滴定实验表明荧光体的电荷转移程度是影响 TICT 发射的主要因素, **1** 是一个新的且其 TICT 发射可以被铜离子调制为“开-关-开”的 TICT 荧光体。

关键词: 分子内扭转电荷转移(TICT); 双重荧光; 铜离子; 配位; “开-关-开”

中图分类号: O614.121 文献标识码: A 文章编号: 1001-4861(2014)09-2181-08

DOI: 10.11862/CJIC.2014.281

Copper(II) Ion Coordination-Controlled Twisted Intramolecular Charge Transfer Dual Fluorescence Emission

ZHANG Jing-Li FAN Wei-Zhen YAN Su-Ting LIN Li-Rong* HUANG Rong-Bin
(College of Chemistry and Chemical Engineering, Xiamen University, Xiamen, Fujian 361005, China)

Abstract: Two twisted intramolecular charge transfer (TICT) fluorophores (**1** and **2**) were designed and synthesized to control the dual fluorescence emission by Cu²⁺ coordination. The dual fluorescence of **2** is quenched upon the addition of Cu²⁺ ions in an “on-off” process similar to PET inhibition. The dual fluorescence of **1** exhibits emission quenching initially and then long-wavelength band (TICT band) emission enhancement with “on-off-on” signalling behaviour. The crystal structure of the Cu²⁺ complex with **1** was also obtained, and its fluorescence properties were reported. ¹H NMR spectral titration results indicate that the degree of charge transfer is a crucial factor for the resulting TICT state emission. Fluorophore **1** is a new TICT compound in which TICT emission can be tuned by copper ions with a dramatic change via “on-off-on” signalling behaviour. CCDC: 899958, Cu²⁺-**1**.

Key words: twisted intramolecular charge transfer; dual fluorescence; copper(II) ion; coordination; “on-off-on” signalling behaviour

0 Introduction

Since Lippert and co-workers first reported the dual fluorescence of 4-(*N,N*-dimethylamino) benzonitrile (DMABN) in the late 1950s^[1], many dual

fluorescence *N,N*-dimethylaniline (DMA) derivatives with electron acceptors at the para position of the donor have been investigated. The two emission bands were assigned to the locally excited (LE) state and the twisted intramolecular charge transfer (TICT) state,

收稿日期: 2014-02-19。收修改稿日期: 2014-04-20。

国家自然科学基金(No.21271150)和国家自然科学基金(No.J1310024)资助项目。

*通讯联系人。E-mail: linlr@xmu.edu.cn; 会员登记号: S06N0582M1006。

where the TICT emission is attributed to a charge separation in an orthogonal rotamer with respect to a C-N linkage between an acceptor group (phenyl ring) and a donor group (dimethylamino group) in the excited states^[2-10]. Although many experimental and theoretical studies have been performed, TICT theory is still controversial and metal coordination control of TICT has remained elusive^[11-24]. There are a few examples in which the cation interacts with the electron-acceptor group of the fluorophore^[23-24]. Generally, the coordination of a transition metal ion with an incomplete d level ($3d^n$, $n < 10$) quenches the fluorescence emission of the fluorophore, usually by electron transfer or energy transfer (on-off signalling behaviour)^[25-31]. Both mechanisms have been observed for Cu^{2+} . TICT fluorophores for Cu^{2+} have also been found with enhanced short-wavelength emission of the LE state at the expense of the long-wavelength TICT emission^[23,32-33]. This phenomenon is similar in principle to photoinduced electron transfer (PET) inhibition (off-on signalling behaviour). Recently, Cu^{2+} was incorporated into the electron acceptor of a TICT fluorophore with a dramatic enhancement of CT fluorescence (off-on signalling behaviour)^[34]. TICT fluorophores with dual fluorescence emitted from two excited states provide a unique opportunity to determine the influence of cation binding on the CT transition^[35-37]. In this study, according to the TICT

mechanism, fluorophores **1** and **2** (Scheme 1) were straight-forward designed based on 4-(*N,N*-dimethylamino)benzamide^[38-39], whose electron acceptor is changed into bis (pyridin-2-ylmethyl)amine, acting as a receptor for Cu^{2+} . Accordingly, the methylene substituent as a structural alteration would affect the dual fluorescence behaviour of the two fluorophores upon binding with Cu^{2+} ions. Thus, the two new TICT dual fluorescent fluorophores show very different signalling responses to Cu^{2+} .

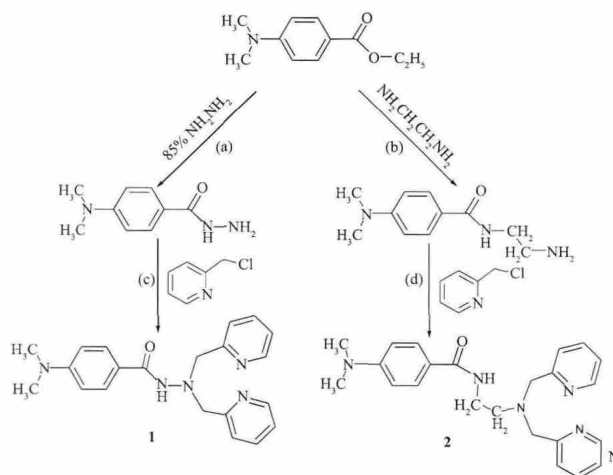
1 Experimental

1.1 Materials

2-(Chloromethyl)pyridine hydrochloride and Ethyl-(dimethylamino)benzoate were purchased from Sigma-Aldrich Chemical Co.. The other chemicals were obtained from Sinopharm Chemical Reagent Ltd. Co. and used as received without further purification. Analytical-grade solvents (Shanghai Chemicals Group Co.) were redistilled before use. Distilled-deionised water was used throughout the experiment.

1.2 Physical Measurements

ESI-MS data were obtained on a Bruker ESQUIRE-3000 Plus LC-MS/MS spectrometer. Absorption spectra were scanned on a Shimadzu UV224012PC absorption spectrophotometer. Fluorescence spectra were recorded on a Hitachi F-7000 spectrofluorometer. The slit of UV-Vis spectra



Scheme 1 Syntheses of **1** and **2**: (a) refluxed, 5 h; (b) refluxed, 24 h; (c) $5 \text{ mol} \cdot \text{L}^{-1}$ NaOH, $\text{CH}_3\text{CH}_2\text{OH}$, refluxed, 4 h; (d) $4 \text{ mol} \cdot \text{L}^{-1}$ NaOH, $\text{CH}_3\text{CH}_2\text{OH}$, refluxed, 15 h

measurements was 1 nm. The fluorescence emission spectra were measured at an excitation wavelength of 300 nm. Both of spectral bandwidths for excitation and emission monochromators were set at 5 nm. ^1H NMR and ^{13}C NMR were acquired on a Bruker Unity 400 MHz spectrometer using TMS as an internal standard. The melting point was determined with a X-4 micromelting point apparatus without correction. The fluorescence quantum yield was determined by using comparative method with quinine sulphate as standard^[40]. The X-ray diffraction data were collected on a Bruker SMART Apex CCD diffractometer equipped with graphite-monochromatic Mo $K\alpha$ ($\lambda = 0.071\ 073$ nm) radiation using an ω scan mode at 293(2) K. The structure was solved using direct methods with SHELXS-97 and refined by full-matrix least-squares calculations with SHELXL-97 based on F^2 ^[41]. All non-hydrogen atoms were located at the calculated positions.

CCDC: 899958, Cu²⁺-1.

1.3 Preparation of 4-(Dimethylamino) benzo-hydrazide^[42]

A mixture of ethyl-4-(dimethylamino)benzoate (10.0 g, 52.0 mmol) and hydrazinium hydroxide (85%, 100 mL) in a round-bottom flask was stirred and refluxed at 120 °C for 5 h. After that, the solution was cooled to room temperature and forming white precipitate which was then filtered off under reduced pressure and washed several times with pure water. The product was recrystallized from ethanol (7.0 g, Yield: 75%). m.p.: 175~177 °C; ^1H NMR (400 MHz, DMSO- d_6), δ 2.98 (s, 6H, CH₃), 4.33 (s, 2H, NH₂), 6.68~6.70 (m, 2H, ArH), 7.69~7.72 (m, 2H, ArH), 9.40 (s, 1H, NH); ESI-MS: m/z Calculated for 179.11, Obsd. 180.2(M+H)⁺.

1.4 Synthesis of 4-(Dimethylamino)-*N'*, *N'*-bis (pyridin-2-ylmethyl)benzohydrazide(1)^[43]

A mixture of 4-(dimethylamino)benzohydrazide (1.6 g, 9.0 mmol) and 2-(chloromethyl)-pyridine hydrochloride (3.2 g, 19.7 mmol), dissolved in mixed solution of 25 mL, 5 mol · L⁻¹ NaOH and 20 mL ethanol, then was stirred and refluxed at 100 °C for 5 h. After that, the resulting solution was cooled to

room temperature and 100 mL of saturated NaOH solution was added to the mixture followed by extraction with CH₂Cl₂ until the CH₂Cl₂ layer was slightly yellow in color. The red solution was washed successively with an aqueous HCl solution (pH =5), saturated brine solution. Then, the CH₂Cl₂ solution was dried over anhydrous MgSO₄ and filtered. Removal of the solution afforded the ligand as a red yellow solid. The red yellow solid was recrystallized with acetic ether/CH₂Cl₂ (1:1, V/V) (2.26 g, Yield: 70%). m.p.: 193~195 °C; ^1H NMR (400 MHz, DMSO- d_6), δ 2.92 (s, 6H, CH₃), 4.27 (s, 4H, CH₂), 6.62 (d, 2H, $J=8.8$ Hz, 2H, ArH), 7.21~7.23 (m, 2H, ArH), 7.53 (d, $J=8.7$ Hz, 2H, ArH); 7.75~7.77 (m, 4H, ArH), 8.46 (d, $J=4.1$ Hz, 2H, ArH), 9.35 (s, 1H, NH). ^{13}C NMR (100 MHz, DMSO- d_6), δ 40.16, 62.45, 111.17, 120.74, 123.18, 129.00, 136.84, 149.14, 152.59, 158.65, 165.66. ESI-MS: m/z Calculated for 361.19, Obsd. 362.2(M+H)⁺.

1.5 Preparation of *N*-(2-aminoethyl)-4-(dimethyl-amino)benzamide

The procedure for preparation of *N*-(2-aminoethyl)-4-(dimethylamino)benzamide is similar with that of 4-(dimethylamino)benzohydrazide. A mixture of ethyl-4-(dimethylamino)benzoate(10.0 g, 52 mmol) and ethane-1,2-diamine(100 mL) was stirred at 120 °C for 48 h. The resulting solution was allowed to cool to room temperature, then the forming yellow precipitate was filtered off under low pressure and washed several times with acetic ether with 70.3% yield. m.p.: 73~74 °C; ^1H NMR (400 MHz, DMSO- d_6), δ 1.46 (bs, 2H, NH₂), 2.66 (d, $J=6.6$ Hz, 2H, CH₂), 2.96 (s, 6H, CH₃), 3.22 (d, $J=5.8$ Hz, 2H, CH₂), 6.69 (d, $J=9.0$ Hz, 2H, ArH), 7.72 (d, $J=9.0$ Hz, 2H, ArH), 8.02 (s, 1H, NH); ESI-MS: m/z Calculated for 207.14, Obsd. 208.2(M+H)⁺.

1.6 Synthesis of *N*-(2-(bis (pyridin-2-ylmethyl) amino)ethyl)-4-(dimethylamino)benzamide(2)

A mixture of *N*-(2-aminoethyl)-4-(dimethylamino)benzamide (1.0 g, 6.1 mmol) and of 2-(chloromethyl)-pyridine hydrochloride (0.58 g, 2.8 mmol), dissolved in 15mL of 5 mol · L⁻¹ NaOH and 15 mL ethanol mixed solution, then was stirred and refluxed at 100 °C for 15 h. After that, the resulting solution was

cooled to room temperature and the mixture was extracted with CH_2Cl_2 until the CH_2Cl_2 layer was slightly yellow in color. The CH_2Cl_2 solution was washed successively with an aqueous HCl solution (pH=5) for seven times, and saturated brine solution for 3 times. And the CH_2Cl_2 solution was dried over anhydrous MgSO_4 and filtered. Removal of the solution afforded the ligand as a yellow liquid. The yellow liquid was chromatographed on silica gel with acetic ether/ $\text{CH}_3\text{CH}_2\text{OH}$ (100:1, V/V) as eluent to give 0.2 g (18.2%) of **2** as a colorless liquid. ^1H NMR (400MHz, DMSO-d_6), δ 2.67 (t, $J=6.5$ Hz, 2H, CH_2), 2.96 (s, 6H, CH_3), 3.43~3.38 (m, 2H, CH_2), 3.81 (s, 4H, CH_2), 6.72 (d, $J=9.0$ Hz, 2H, ArH), 7.23 (ddd, $J=7.4, 4.9, 1.0$ Hz, 2H, ArH), 7.53 (d, $J=7.8$ Hz, 2H, ArH); 7.67 (td, $J=7.6, 1.6$ Hz, 2H, ArH), 7.75 (d, $J=8.8$ Hz, 2H, ArH), 8.15 (s, 1H, NH), 8.47 (d, $J=4.0$ Hz, 2H, ArH). ^{13}C NMR (100 MHz, DMSO-d_6), δ 36.71, 53.58, 59.49, 73.64, 111.27, 121.65, 122.39, 123.21, 128.88, 137.12, 149.18, 152.86, 158.70, 166.70. ESI-MS: m/z Calculated for 389.22, Obsd. 390.7 ($\text{M}+\text{H}$) $^+$.

2 Results and discussion

The fluorescence measurements of the two TICT fluorophores were performed in representative solvents of different polarity, as shown in Fig.1. As expected, these two fluorophores emit typical dual fluorescence in normal polar solvents, such as methanol, ethanol, acetonitrile and dichloromethane. The influence of Cu^{2+} ions from copper (II) nitrate on the dual fluorescence of the two fluorophores was investigated, and their dual fluorescence behaviour response to Cu^{2+} was expected to be different.

Fig.2 shows that, upon the addition of Cu^{2+} ions, the variation of the dual fluorescence of **1** (quantum yield=0.022 in acetonitrile) is very different from that of **2** (quantum yield =0.013 in acetonitrile). The dual fluorescence maxima of **2** at 363 nm and 492 nm are quenched upon the addition of Cu^{2+} ions in an “on-off” process similar to PET inhibition. In contrast, the dual fluorescence maxima of **1** at 372 nm and 498 nm are initially quenched upon the addition of Cu^{2+} ions in an

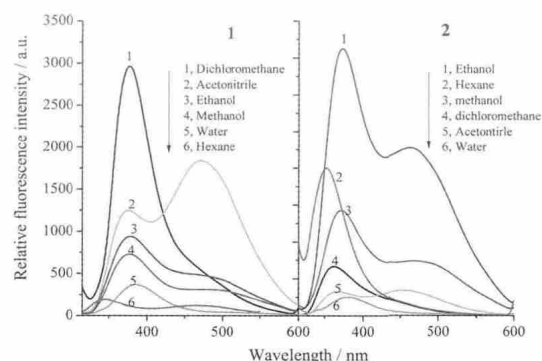


Fig.1 Dual fluorescence spectra of **1** ($5.0 \times 10^{-5} \text{ mol} \cdot \text{L}^{-1}$, left) and **2** ($5.0 \times 10^{-5} \text{ mol} \cdot \text{L}^{-1}$, right) in different solvents

“on-off” process. The long band at 416 nm then appeared and was enhanced in an “off-on” process upon the addition of more Cu^{2+} ions, whereas the short-wavelength band at 372 nm plateaued. Other Cu^{2+} compounds, such as CuSO_4 , CuCl_2 , $\text{Cu}(\text{ClO}_4)_2$, yielded the same results. That is, **1** shows “on-off-on” signalling behaviour controlled by Cu^{2+} coordination. This behaviour is different from that of previously reported TICT fluorophores for Cu^{2+} , for which the LE emission was greatly enhanced upon Cu^{2+} binding whereas the TICT emission was quenched or the LE emission changed only slightly whereas the TICT emission was dramatically enhanced and blue-shifted^[23,34].

The total fluorescence intensity of **1** in aqueous acetonitrile solution is independent of the aqueous phase pH value over 5~12 (Fig. S1 in Supporting Information); therefore, all experiments were performed in an acetonitrile/water mixed solution (1:1, V/V). The response of fluorophore **1** toward a variety of other metal ions, namely, Pb^{2+} , Zn^{2+} , Hg^{2+} , Ni^{2+} , Ag^+ , Co^{2+} , Cd^{2+} , Mn^{2+} , Ca^{2+} , Fe^{3+} , Al^{3+} , K^+ , Na^+ , and Mg^{2+} , was also examined in the acetonitrile/water solution. As expected, these metal ions simply quenched the fluorescence to differing extents (see Fig.S2 in SI). Meanwhile, the dual fluorescence of **1** in the presence of two equivalents of Cu^{2+} was barely affected by the coexistence of six equivalents of other metal ions (Fig. 3). This finding indicates that fluorophore **1** shows a special and highly selective dual fluorescence response toward Cu^{2+} .

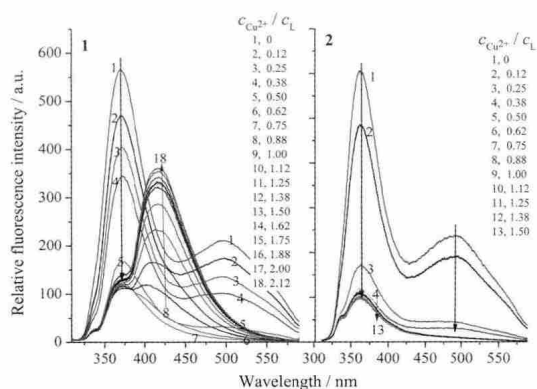


Fig.2 Evolution of fluorescence spectra during the titration of **1** ($5.0 \times 10^{-5} \text{ mol} \cdot \text{L}^{-1}$, left) and **2** ($5.0 \times 10^{-5} \text{ mol} \cdot \text{L}^{-1}$, right) with Cu^{2+} in acetonitrile/water (1:1, V/V) solution

To understand the effect of Cu^{2+} on the dual fluorescence of fluorophore **1**, the evolution of the fluorescence spectra as a function of the ratio of Cu^{2+} concentration to **1** (Fig. S3 in SI) was studied. The results revealed that the dual fluorescence emission of **1** decreased dramatically before the amount of Cu^{2+} reached one equivalent of **1**, after which the substantially shifted long band was observed and enhanced by the addition of more Cu^{2+} , whereas the short band did not change. Furthermore, when **2** equivalents of Cu^{2+} were added, the intensity of the dual fluorescence plateaued.

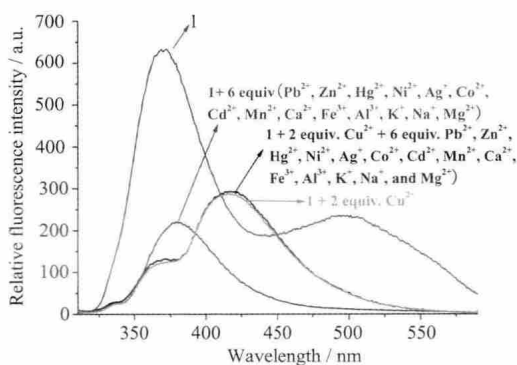


Fig.3 Fluorescence spectra of **1** ($5.0 \times 10^{-5} \text{ mol} \cdot \text{L}^{-1}$) in the absence and presence of **2** equiv. of Cu^{2+} and **2** equiv. of Cu^{2+} plus 6 equiv. of other metal ions in acetonitrile/water (1:1, V/V) solution, respectively

The absorption spectra of **1** in the presence of different concentrations of Cu^{2+} ions are also scanned (shown in Fig.S4). When increasing amounts of Cu^{2+} ions were introduced into an $\text{CH}_3\text{CN}/\text{H}_2\text{O}$ (1:1, V/V)

solution, the absorbance peak centred at 307 nm of **1** ($\epsilon_{307} = 3.6 \times 10^4 \text{ L} \cdot \text{mol}^{-1} \cdot \text{cm}^{-1}$) was gradually red shifted to 324 nm and then increased with an isosbestic point at 310 nm. The plot of the absorbance intensity at 324 nm versus the concentration ratio of Cu^{2+} ions to **1** (Fig.4a) indicated that **1** binds with Cu^{2+} ions in a 1:1 stoichiometry.

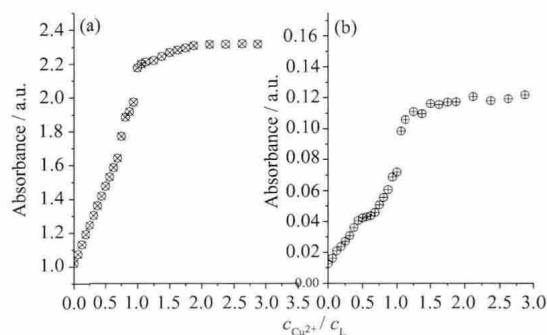
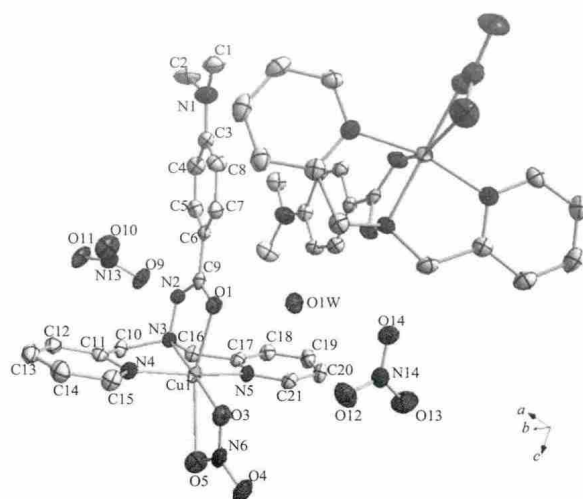


Fig.4 Absorbance intensity at 324 nm (a) and 420 nm (b) as a function of the concentration ratio of Cu^{2+} to **1** ($c_1 = 5.0 \times 10^{-5} \text{ mol} \cdot \text{L}^{-1}$)

To ascertain the binding mode of Cu^{2+} with **1**, the complex of **1** with Cu^{2+} was also obtained. The X-ray quality crystals of Cu^{2+} -**1** complex were easily obtained by slow evaporation from the 1:1 (molar ratio) mixed solution of $\text{Cu}(\text{NO}_3)_2$ with **1** in acetonitrile and an X-ray crystal structure analysis was performed, as shown in Fig.5. The Cu^{2+} -**1** complex crystallizes in monoclinic system, space group $P2_1/c$ with $a = 0.8710(1) \text{ nm}$, $b = 1.3843(2) \text{ nm}$, $c = 3.9223(6) \text{ nm}$, $\alpha = 90^\circ$, $\beta = 96.193(2)^\circ$, $\gamma = 90^\circ$, $V = 4.7016(11) \text{ nm}^3$, $Z = 4$, Formula weight = 1116.02, $D_c = 1.58 \text{ g} \cdot \text{cm}^{-3}$, $\mu = 0.990 \text{ mm}^{-1}$, $F(000) = 2303.4$ at $T = 273(2) \text{ K}$ and 25540 reflections were measured, 9233 unique ($R_{\text{int}} = 0.041$), 8036 ($I > 2\sigma(I)$) which were used in all calculations with final $R = 0.058$. The asymmetric unit has two independent molecules and one free water molecule. The Cu^{2+} cation chelates to **1** with the pyridine N, the carbonyl O and the hydrazide N and binds the two O atoms of nitrate to form a six-coordinate octahedral arrangement. This cation is counterbalanced by one nitrate anion. The coordination of Cu^{2+} leads to a lengthening of the C=O bond (0.123 nm) and a shortening of the C-N bond (0.134 nm) and the C(9)-C(6) bond (0.147 nm)^[44-45]. At the electron-donor side,



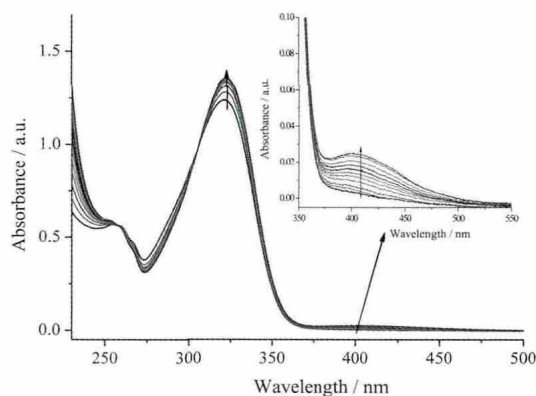
Hydrogen atoms are removed for clarity

Fig.5 Thermal ellipsoid plot of the Cu^{2+} complex with **1** at the 50% probability level

the twisted angle between the plane through C (2), C (1), and N(1) of the dimethylamino group and that of the phenyl ring amounts to $15.23^\circ(0.59)$.

The fluorescence spectra of the Cu^{2+} complex (quantum yield $\Phi=0.019$ in acetonitrile) show only one band at the same wavelength in both the solid state and solution (Fig. S5 in SI), giving strong support for the dual fluorescence of **1** evolving in the presence of Cu^{2+} before the amount of Cu^{2+} reached one equivalent of **1**. The next question is why the long-band fluorescence enhancement and blue shift were observed upon after Cu^{2+} ions exceeding one equivalent of **1** were added. When further examining the nature of the interaction between the Cu^{2+} ions and **1**, it was found that the absorption peak centred at 420 nm suddenly appeared and then increased in intensity when the concentration of Cu^{2+} ions exceeded one equivalent of **1** (Inset of Fig. 6). As shown in Fig.4b, the plot of the absorbance intensity at 420 nm versus the concentration ratio of Cu^{2+} ions to **1** exhibits an Γ -shaped like curve with a break point at the 1.0 ratio. That is, the Cu^{2+} ions interacted with the formation of the Cu^{2+} -**1** complex when a greater amount of Cu^{2+} was introduced. Thus, greater amounts of Cu^{2+} affected the Cu^{2+} -**1** complex, not just **1**. This assumption was further supported by the absorption titration of the Cu^{2+} -**1** complex with Cu^{2+} ions in $\text{CH}_3\text{CN}/\text{H}_2\text{O}$ solution (1 :1, V/V), in which the

absorption spectra of the Cu^{2+} -**1** complex varied with the concentration of Cu^{2+} ions (Fig.6). When an increasing concentration of Cu^{2+} ions was introduced into the $\text{CH}_3\text{CN}/\text{H}_2\text{O}$ solution of the Cu^{2+} -**1** complex, the band at 324 nm ($\epsilon_{324}=3.6\times 10^4 \text{ L}\cdot\text{mol}^{-1}\cdot\text{cm}^{-1}$) was attenuated and a new peak at 420 nm appeared. A plot of the absorbance intensity at 324 nm versus the concentration of Cu^{2+} ions, after non-linear fitting assuming a 1:1 stoichiometry, yielded a $1.6\times 10^5 \text{ L}\cdot\text{mol}^{-1}$ binding constant with a R^2 value of 0.996 1 (Fig. S6 in SI). This effect is perhaps related to the amino nitrogen of the donor group complexed with the Cu^{2+} ion^[37,46]. (The effect of Cu^{2+} itself to the absorption spectra was



Inset: magnified spectra between 300 nm and 500 nm

Fig.6 Evolution of UV-visible absorption spectra during the titration of the Cu^{2+} complex ($5.0\times 10^{-5} \text{ mol}\cdot\text{L}^{-1}$) with increasing Cu^{2+} concentration

excluded by checking its absorbance in the used concentration range.)

^1H NMR experiments were performed in $\text{CD}_3\text{CN}/\text{D}_2\text{O}$ (1:1, V/V) solution to further classify this TICT mechanism. As Cu^{2+} is paramagnetic, some of NMR signals near the centre of coordinated Cu^{2+} were absent whereas those far from the Cu^{2+} centre were present and the H_{as} , H_{gs} , and H_{e} protons in acceptors experienced downfield shifts upon the addition of one equivalent of Cu^{2+} ions, whereas H_{h} , located in the dimethylamino donor site, shifted upfield (Fig.7). The downfield shifts of the H_{a} (from 9.19 to 10.80), H_{g} (from 7.40 to 7.87) and H_{e} (from 3.68 to 3.91) protons signals are due to the decrease in the electron density by the coordination of Cu^{2+} at the acceptor sites. H_{h} in the dimethylamino donor site firstly showed a downfield shift (from 2.75 to 2.78) and then an upfield shifts (from 2.78 to 2.69), indicating that H_{h} hydrogens experienced an increase in electron density. When a concentration of Cu^{2+} ions exceeding one equivalent of **1** was introduced, the slight upfield shifts observed also indicate that the coordination effect of Cu^{2+} ions with nitrogen at the dimethylamino donor weakened the upfield shifts. Thus, the formation of the Cu^{2+} -**1** complex affected the electronic structure properties of fluorophore **1** in the ground state and efficient PET in the excited state may occur due to the increased degree of charge separation between the donor and acceptor. Thus, the TICT states of the rotors did not cause any fluorescence emission of

1, leading to the absence of long-band fluorescence emission of the Cu^{2+} -**1** complex. However, the H_{as} , H_{gs} , H_{e} and H_{h} protons in acceptor and donor sites all experienced upfield shifts upon the addition of more than a stoichiometric amount of Cu^{2+} ions, which reduces the degree of charge separation between the donor and acceptor and the retardation of PET. Thus, the long-band fluorescence enhancement and blue shift were observed after the concentration of Cu^{2+} ions exceeded one equivalent of **1**. The blue-shifted TICT emission in the presence of a greater-than-stoichiometric amount of Cu^{2+} ions actually indicated an enlarged energy gap between the emissive TICT state and its corresponding ground state and the results of a decreased radiationless rate constant^[47]. The NMR results indicate that the degree of charge transfer is a crucial factor in the resulting TICT state^[48].

3 Conclusions

In summary, two fluorophores (**1** and **2**) were designed and synthesised to control the dual fluorescence emission by Cu^{2+} coordination according to the TICT mechanism. Fluorophore **2** is a normal TICT compound in which dual fluorescence is quenched by Cu^{2+} ions in an “on-off” process similar to PET inhibition. The dual fluorescence of fluorophore **1**, on the other hand, shows “on-off-on” signalling behaviour with response to Cu^{2+} ions. The fluorescence properties of the Cu^{2+} -**1** complex, ^1H NMR spectral titration experimental results demonstrate that the degree of charge transfer is a crucial factor for the resulting TICT state emission. To our best knowledge, fluorophore **1** is the first TICT compound in which TICT emission can be tuned by copper ions with a dramatic change via on-off-on signalling behaviour. **1** is a unique molecule exhibiting a new mechanism via “on-off-on” dual fluorescence of a highly selective response toward Cu^{2+} ions. This TICT characteristic might provide a new strategy for further development of new “on-off-on” TICT fluorophores and helps further explain TICT emission mechanism.

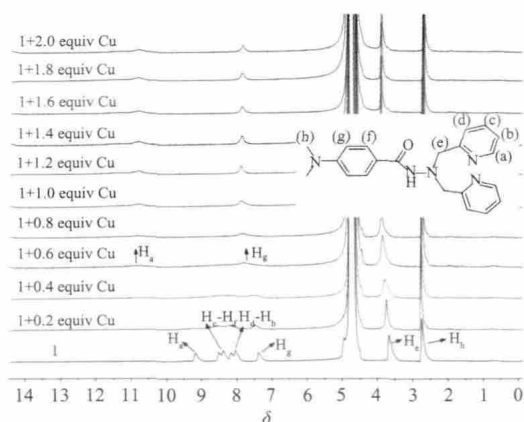


Fig.7 ^1H NMR spectra of **1** in the presence of different concentrations of Cu^{2+} ions in $\text{CD}_3\text{CN}/\text{D}_2\text{O}$ (1:1, V/V) mixed solution

Acknowledgments: We are grateful to the financial

support of the National Natural Science Foundation of China (Grant No. 21271150) and NFFTBS (Grant No. J1310024).

Supplementary data associated with this article can be found in the online version, at DOI: 10.11862/CJIC.2014.281.

References:

- [1] Lippert E, Lüder W, Moll F, Nägele W, et al. *Angew Chem.*, **1961**,**73**:695-706
- [2] Coley D J, Peoples A H. *J. Chem. Soc. Chem. Commun.*, **1977**,**10**:352-353
- [3] Grabowski Z R, Rotkiewicz K, Siemiarczuk A. *Nouv. J. Chim.*, **1979**,**3**:443-454
- [4] Rettig W. *Angew. Chem. Int. Ed.*, **1986**,**25**:971-988
- [5] Rettig W, Chandross E A. *J. Am. Chem. Soc.*, **1985**,**107**:5617-5624
- [6] Vogel M, Rettig W, Heimbach P. *J. Photochem. Photobiol., A*, **1991**,**61**:65-75
- [7] Revill JAT, Brown R G. *J. Fluor.*, **1992**,**2**:107-115
- [8] Zachariasse K A, Grobys M, Von der Haar T, et al. *J. Photochem. Photobiol., A*, **1996**,**102**:59-70
- [9] Lin L R, Yang W L, Zheng G L, et al. *Spectrochim. Acta: Part A*, **2004**,**60**:2209-2213
- [10] Ito A, Ishizaka S, Kitamura N. *Phys. Chem. Chem. Phys.*, **2010**,**12**:6641-6649
- [11] Köhler G, Rechthaler K, Grabner G, et al. *J. Phys. Chem. A*, **1997**,**101**:8518-8525
- [12] Dreyer J, Kummrow A. *J. Am. Chem. Soc.*, **2000**,**122**:2577-2585
- [13] Mennucci B, Toniolo A, Tomasi J. *J. Am. Chem. Soc.*, **2000**,**122**:10621-10625
- [14] Kwok W M, Ma C, Phillips D, et al. *J. Phys. Chem. A*, **2000**,**104**:4188-4197
- [15] Dobkowski J, Wójcik J, Komiński W, et al. *J. Am. Chem. Soc.*, **2002**,**124**:2406-2407
- [16] Yang J S, Liao K L, Wang C M, et al. *J. Am. Chem. Soc.*, **2004**,**126**:12325-12335
- [17] Amatatsu Y. *J. Phys. Chem.*, **2006**,**110**:8736-8743
- [18] Zachariasse K A, Druzhinin S I, Galievsky V A, et al. *J. Phys. Chem.*, **2010**,**114**:13031-13039
- [19] Galván I F, Martín M E, Aguilar M A. *J. Chem. Theory Comput.*, **2010**,**6**:2445-2454
- [20] Chipem F A S, Mishra A, Krishnamoorthy G. *Phys. Chem. Chem. Phys.*, **2012**,**14**:8775-8790
- [21] Krishnamoorthy G, Dogra S K. *J. Phys. Chem. A*, **2000**,**104**:2542-2551
- [22] Morozumi T, Anada T, Nakamura H. *J. Phys. Chem. B*, **2001**,**105**:2923-2931
- [23] Malval J P, Lapouyade R. *Helv. Chim. Acta*, **2001**,**84**:2432-2451
- [24] Aoki S, Kagata D, Shiro M, Takeda K, et al. *J. Am. Chem. Soc.*, **2004**,**126**(41):13377-13390
- [25] Torrado A, Walkup G K, Imperiali B. *J. Am. Chem. Soc.*, **1998**,**120**:609-610
- [26] Valeur B, Leray I. *Coord. Chem. Rev.*, **2000**,**205**:3-40
- [27] Li Y, Yang C M. *Chem. Commun.*, **2003**,**23**:2884-2885
- [28] Zhou Y, Wang F, Kim Y, et al. *Org. Lett.*, **2009**,**11**:4442-4445
- [29] Varnes A W, Dodson R B, Wehry E L. *J. Am. Chem. Soc.*, **1972**,**94**(3):946-950
- [30] Prodi L, Bolletta F, Montaldi M, et al. *Eur. J. Inorg. Chem.*, **1999**,**3**:455-460
- [31] Mokhir A, Kiel A, Hertel D P, et al. *Inorg. Chem.*, **2005**,**44**:5661-5666
- [32] Rurack K, Kollmannsberger M, Resch-Genger U, et al. *J. Am. Chem. Soc.*, **2000**,**122**(5):968-969
- [33] Xu Z, Xiao Y, Qian X, et al. *Org. Lett.*, **2005**,**7**:889-892
- [34] Wen Z C, Yang R, He H, et al. *Chem. Commun.*, **2006**,**1**:106-108
- [35] Kim J, Morozumi T, Nakamura H. *Tetrahedron*, **2008**,**64**:10735-10740
- [36] Upadhyay K K, Kumar A. *Org. Biomol. Chem.*, **2010**,**8**:4892-4897
- [37] Li Q, Peng M, Li H, et al. *Org. Lett.*, **2012**,**14**:2094-2097
- [38] Braun D, Rettig W, Delmond S, et al. *J. Phys. Chem. A*, **1997**,**101**:68366841
- [39] Wu F Y, Jiang Y B. *Chem. Phys. Lett.*, **2002**,**355**:438-444
- [40] Lakowicz J R. *Principles of Fluorescence Spectroscopy. 2nd Edition*. New York: Kluwer Academic/Plenum Press, **1999**.
- [41] Sheldrick G M. *SHELXS 97 and SHELXL 97, Program for Crystal Structure Solution*. University of Göttingen: Germany, **1997**.
- [42] Ma J, Fan W Z, Lin L R. *Acta Cryst.*, **2011**,**E67**:m624-m625
- [43] Eroy-Reveles A A, Leung Y, Beavers C M, et al. *J. Am. Chem. Soc.*, **2008**,**130**:4447-4458
- [44] Vargas R, Garza J, Dixon D, et al. *J. Phys. Chem. A*, **2001**,**105**:774-778
- [45] Bera H, Dolzhenko A V, Tan G K, et al. *Acta Cryst.*, **2010**,**E66**:o1241
- [46] Das T, Kumar A, Ghosh P, et al. *J. Phys. Chem. C*, **2010**,**114**:19635-19640
- [47] Badugu R, Lakowicz J R, Geddes C D. *J. Am. Chem. Soc.*, **2005**,**127**:3635-3641
- [48] Zhao G J, Yu F, Zhang M X, et al. *J. Phys. Chem. A*, **2011**,**115**:6390-6393